A 144 GHz 2.5mW Multi-Stage Regenerative Receiver for mm-Wave Imaging in 65nm CMOS

Adrian Tang, Zhiwei Xu, Qun Jane Gu, Yi-Cheng Wu, and Mau Chung Frank Chang

***Abstract*—This paper introduces the multi-stage regenerative receiver, an architecture that extends the super-regenerative receiver beyond the classical single-stage configuration to achieve higher gain and sensitivity. This makes the receiver ideal for mm-wave imaging by relaxing the required illumination power in the link budget. The receiver is implemented in 65nm CMOS and achieves a sensitivity of -74 dBm, a NF of 10.2 dB, consumes 2.5mW of power and occupies 0.02mm^2 of chip area.**

I. INTRODUCTION

Recently emerging applications in security screening have created an increased interest in active mm-wave imaging throughout the circuit community. While mm-wave imaging systems has been commercialized successfully in III-V GaAs and SiGe HBT technologies, CMOS based imaging systems have had limited impact due to the low output power associated with CMOS devices operating at mm-wave imaging frequencies (>94 GHz). CMOS imaging however, offers several unique advantages over III-V technologies, including much lower operating power, the ability to create low-cost fully integrated pixel arrays, and a considerable reduction in pixel area.

The most challenging system issue faced by CMOS active mm-wave imaging systems is the limited source power available from CMOS for illumination of the target to be imaged. In particular, this limited power becomes difficult for implementing active back-scattering mm-wave imagers (imaging systems that shine mm-wave signals at the target and then measure the reflected power). This is because in back-scattering systems the signal must first travel to the target, and then reflect back to the imaging system. This results in much higher path loss than regular communication radio links where the signal travels in only one direction, from transmitter to receiver.

Fig.1 shows the simplified link budget for a typical security screening imager system. Since the signal must travel in both directions, the free space path loss of back-scattering is about double that of a typical radio link budget (in dB). Also since the target materials involved in security screening (clothing, skin, and plastic) have very low reflection coefficients, the situation is exacerbated because almost all the source power is lost in the reflection process. Loosing 80-90dB of signal power to path loss and reflection is typical in a security screening system. To overcome this difficult link budget, commercial mm-wave imaging systems typically employ high power III-V sources in the range of 30 dBm (1 W) to provide illumination

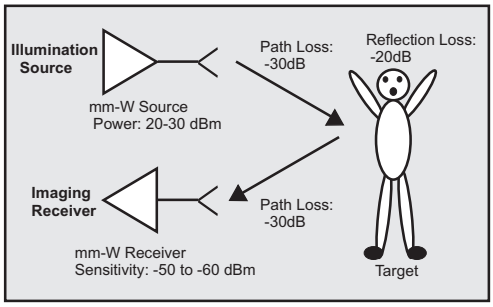

Fig. 1. Simplified link budget of a typical back-scattering mm-wave imager system for security screening.

of the target. While this "brute force" solution does balance the link budget, such an approach is not practical for CMOS based mm-wave imaging where output power is limited to < 15 dBm in state-of-art imaging mm-wave sources (>94 GHz) [1],[2],[3].

Instead of increasing the source power, an alternative solution is to increase the receiver sensitivity, allowing it to detect smaller signals. This relaxes the source power requirements while still keeping the link budget balanced. Modern CMOS mm-wave receivers for communications are typically based on heterodyne or direct conversion topologies that can achieve sensitivities approaching -65 dBm, which is consistent with the current link budget and still requires source power in the 25-35 dBm range. In this paper, we propose the multi-stage regenerative receiver, a receiver which extends the classical super-regenerative architecture into a multiple-stage configuration in order to achieve higher sensitivity than is possible with either heterodyne or direct conversion receiver architectures. This higher sensitivity allows the source power requirement of a mm-wave imaging system to be lowered to the point where an all- CMOS imaging system becomes feasible.

II. SUPER-REGENERATIVE RECEIVERS

The Super-regenerative receiver (SRR) offers a simpler architecture, lower power consumption, and higher sensitivity than its heterodyne and direct conversion counterparts. SRR receivers are able to achieve higher sensitivity because they operate based on oscillatory amplification instead of the tuned amplification. Oscillatory or "regenerative" amplification can achieve very high Q factors leading to much lower receiver bandwidth than is possible with low noise amplifier (LNA) based heterodyne and direct conversion receivers. Lower receiver bandwidth directly translates into better sensitivity for

978-1-4244-8292-4/11/$26.00 ©2011 IEEE

a fixed noise figure (NF). The sensitivity of a receiver can be approximated using the Rayleigh-Jean model of thermal noise:

$$S = KTB(NF).$$

Where B is the receiver bandwidth, K is the Boltzmann constant and T is the temperature in Kelvin. Unlike mm-wave receivers for communications where large bandwidth (GHz range) is desired to support high data rates, imaging systems do not suffer from a lowered bandwidth as video frame rates are on the order of 100 Hz.

While SRRs are sometimes used for low-cost and low-speed ASK data receivers [4], their non-coherent nature has severely limited their use in mm-wave communications as they are unable to recover phase information needed for the quadrature modulation used by nearly all modern data links. Retaining the phase information has no value for mm-wave imaging since the total received power is used to construct the image, not the phase. This makes SRR receivers an excellent architecture for mm-wave imaging applications [5]. SRR receivers also have an extremely non-linear response in which the output voltage is logarithmically proportional to input power. While this highly compressive behavior is undesirable for communication systems where any severe non-linearity will introduce inter-modulated distortion, it is actually beneficial for imaging as operation as the log response improves the dynamic range of the detector. Additionally inter-modulation is not a concern for imaging which is usually performed at a single frequency.

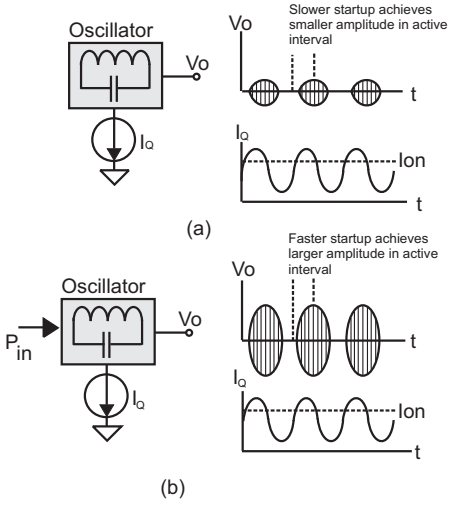

Fig. 2. Operation of classic super-regenerative receiver. (a) Time-domain waveforms without an injected signal. (b) Time-domain waveforms when power P_{in} is injected at the oscillator fundamental frequency.

The block diagram of the classic super-regenerative receiver is shown in Fig.2a. The operation of the super-regenerative receiver operates as follows: An oscillator is periodically turned on and off by a time varying current source I_Q, commonly called a quench signal (as it quenches the oscillations out of the receiver). When the quench current I_Q is larger than I_{on} the oscillator has enough gain to sustain oscillation, when I_Q falls below I_{on} the oscillation is not sustained. This results in the a voltage waveform at the oscillator output which has an envelope modulated by I_Q. As shown in Fig.2b, when power is injected into the oscillator at the fundamental frequency, the start-up time of the oscillator is reduced, allowing the output voltage to reach higher amplitudes for the same "on" period of I_Q. Finally, by tracking the amplitude of the oscillator an estimation of the injected power is made. The power estimation is usually accomplished with an envelope detector and low-pass filter. Unlike typical receiver LNA stages which can readily be cascaded to increase RF amplification, there are several characteristics of the super-regenerative operation which render it impossible to directly cascade multiple stages to achieve higher gain or higher sensitivity:

- The output frequency is different than the input frequency. The input frequency is at the fundamental of the oscillator while the output frequency is the same as the quench signal I_Q.
- The super-regenerative receiver is a time varying system. The receiver is most sensitive to the input at the instant the oscillator is started, while the maximum output voltage occurs at the instant the oscillator envelope has grown to a maximum.

III. Multi-Stage Regenerative Receivers

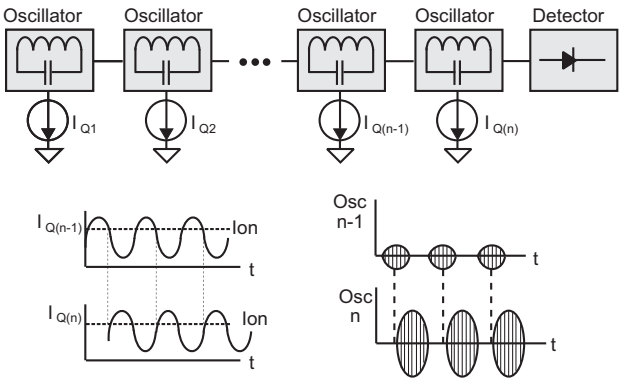

Fig. 3. Proposed multi-stage regenerative receiver architecture and time domain waveforms.

Based on the above considerations we propose a multi-stage regenerative architecture that can be formed by cascading regenerative receivers and correctly adjusting the phase of each stage's quench signal as shown in Fig.3. In this topology the second stage oscillator is engaged in the middle of the first stage's start-up period. Therefore the second stage samples the RF envelope of the first stage, to provide further regenerative amplification. In order to successfully achieve cascaded amplification, the phase relation between the $I_{Q(n-1)}$ and $I_{Q(n)}$ has several important constraints for correct operation. The first is that $I_{Q(n)}$ must positively cross I_{on}, at some time during the period where the prior stage oscillator is already active. The signal will not be transferred if the second stage samples when the first stage is off. However if the first stage oscillator is allowed to reach full swing before the second stage samples, the signal will also not be transferred since the

envelope of the first oscillator becomes independent of its input signal once fully started. Fig.4 illustrates these conditions. If $I_{Q(n)}$ positively crosses I_{on} at $(t < t_{on})$ or $(t > t_{sat})$ then no information is contained. Only during the start-up time $(t_{on} < t < t_{sat})$ does the first stage envelope contain input dependence that can be transferred to the second stage.

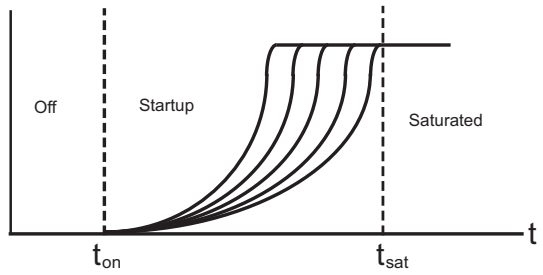

Fig. 4. Start-up voltage envelope of a regenerative oscillator.

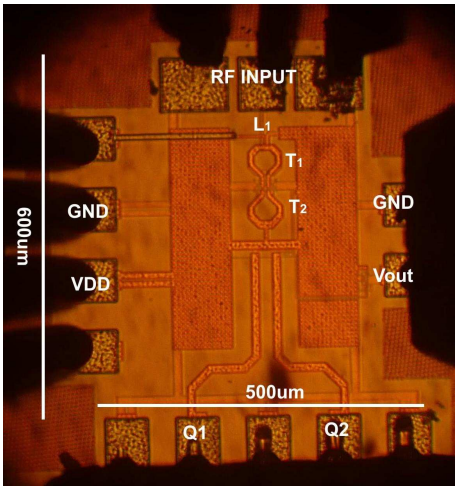

Fig. 6. Die photo of the proposed multi-stage regenerative receiver and probe connections.

IV. Measurement Results

The proposed receiver architecture was used to implement a two-stage regenerative receiver in 65nm CMOS technology. The detailed schematic of the receiver is shown in Fig.5. The quench signal for each stage of the receiver is provided externally so that the phase can be precisely varied for measurement purposes. As the regenerative receiver can be operated with a quench frequency anywhere in the low GHz to low MHz range, an on-chip op-amp based phase shifter can be implemented without difficulty.

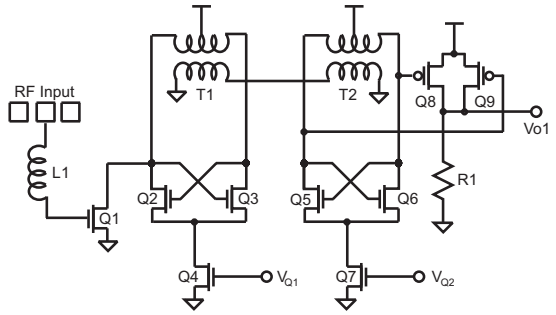

Fig. 5. Circuit implementation of proposed multi-stage regenerative receiver.

Transistor Q1 with input matching line L1 form an input stage which injects the received RF signal directly into the first oscillator formed by Q2, Q3 and transformer T1. The quench for this stage is controlled at the gate of current source Q4 by voltage V_{Q1}. The secondary winding of T1 is used to couple to the second stage transformer T2. Devices Q5 and Q6 provide the negative resistance for the second stage oscillator, with the second stage quench controlled by the voltage V_{Q2} at the gate of Q7. Q8, Q9 and R1 form a simple envelope detector which tracks the amplitude of the second stage oscillator. The die photo of the two-stage regenerative receiver is shown in Fig.6. For testing a GSG waveguide probe input was used to inject the RF signal into the receiver. The entire test structure occupies an area of 0.3 mm^2, while the area of receiver excluding the pads and pad routing (this would represent the pixel area in an array) occupies only 0.02mm^2.

To first characterize the gain of the proposed receiver an input tone at 1dB above the sensitivity level of -73dBm was swept from 143 to 145 GHz and the resulting gain was plotted in Fig.7. The quench signal frequency was set to 10 MHz and the phase offset between V_{Q1} and V_{Q2} was optimized for the point of best sensitivity (48.6 degrees). For super- regenerative receivers the full gain only occurs at the sensitivity level and rapidly decreases above due to its compressive logarithmic shape.

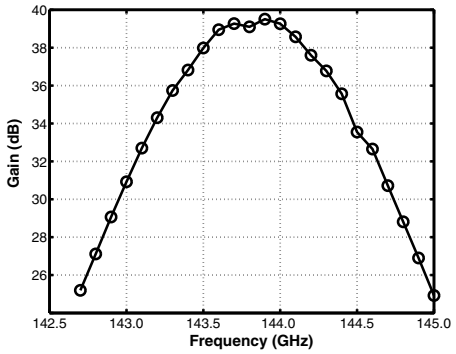

Fig. 7. Output voltage of the proposed multi-stage regenerative receiver as a -73dBm tone is swept through the receiver bandwidth.

To characterize the linearity or power profile of the proposed receiver an input tone of 144 GHz was swept from sensitivity level (-74dBm) up to 0 dBm at the output was voltage was recorded in Fig.8. Clearly visible is the very nonlinear response characteristic of regenerative receivers which compress immediately as the input power departs from the sensitivity level. This was again performed with a 10 MHz quench signal and sensitivity optimized phase between V_{Q1} and V_{Q2}.

To demonstrate the effect of phase between the two quench signals V_{Q1} and V_{Q2} on the gain of the receiver, an external phase shifter between the two stages is varied from 0 to

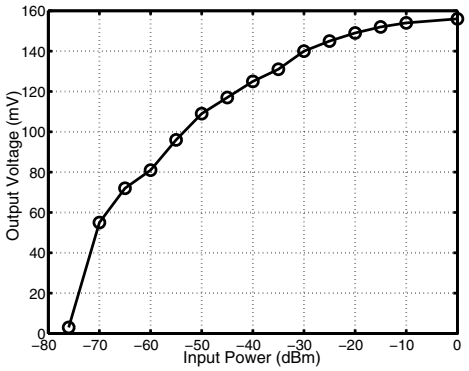

Fig. 8. Output voltage of the proposed multi-stage regenerative receiver as a 144 GHz tone is swept from sensitivity level to saturation level.

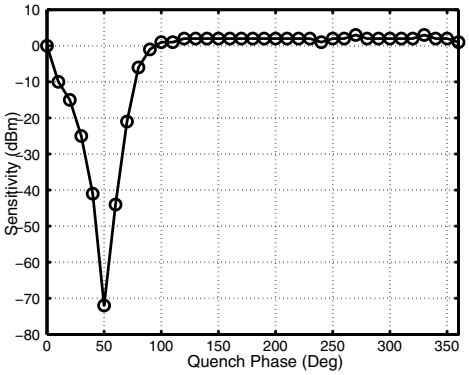

Fig. 10. Sensitivity of the proposed multi-stage regenerative receiver as the phase between stage the 1 and stage 2 quench signal is varied from 0 to 360 degrees.

360 degrees and the gain is measured for each phase setting. Again this was done with a 10 MHz quench frequency. The resulting gain is plotted in Fig.9. Clearly visible is the optimum phase setting at approximately 50 degrees. Note this optimum will be dependent on the quenching frequency. Also note outside the small range around this optimum the proposed receiver exhibits no gain at all as the envelope is not correctly transferred from stage 1 to stage 2. At these phases stage 1 acts as an attenuator placed in front of stage 2 which acts like a single-stage SRR.

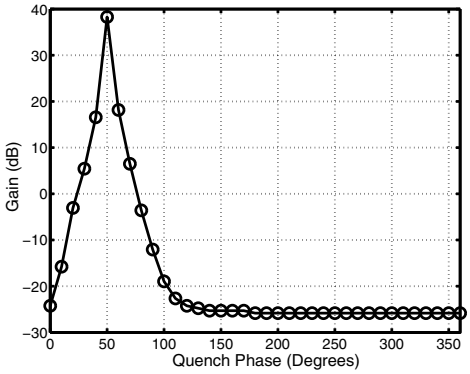

Fig. 9. Gain of the proposed multi-stage regenerative receiver at sensitivity level as the phase between stage the 1 and stage 2 quench signal is varied from 0 to 360 degrees.

Finally Fig.10 plots the sensitivity as the 10 MHz quench signal phase is adjusted from 0 to 360 degrees. Clearly visible the sensitivity again peaks at an optimum value of approximately 50 degrees with -74dBm sensitivity. Note that at phases where the receiver has no gain its sensitivity level well become equal to the peak amplitude of stage 1 as an injected signal must be larger than the oscillation amplitude to disturb the conditions of stage 2. From the sensitivity and bandwidth measurements the noise figure can be computed directly from the equation in section II. The noise figure was found to be 10.2 dB. The noise-equivalent power can also be computed from $S/\sqrt{B}$ and was found to be 1.3fW/Hz$^{0.5}$.

V. Conclusions

The measured performance of the proposed multi-stage regenerative receiver is listed in table I along with a comparison to other state-of-art mm-wave imaging receivers. Measurements have demonstrated that the proposed multi-stage regenerative receiver exhibits a much higher sensitivity, making it ideal for CMOS active mm-wave imaging applications in which large source power for target illumination is not available.

TABLE I
PERFORMANCE OF PROPOSED MULTI-STAGE REGENERATIVE RECEIVER.

Receiver	[6]	[7]	[8]	This work
Frequency (GHz)	94	94	94	144
NEP fW/Hz$^{0.5}$	200	N/A	10.4	1.3
Sensitivity (dBm)	-51	-66	-57	-74
Die Area (mm^2)	0.41	0.31	1.25	0.021
Power Consumption (mW)	39.6	93	200	2.5

References

[1] Laskin, E. Chevalier, P. Chantre, A. Sautreuil, B. Voinigescu, S.P. , 80/160-GHz Transceiver and 140-GHz Amplifier in SiGe Technology, *IEEE RFIC*, Jun. 2007, pp 153-156.

[2] Sandstrom, D. Varonen, M. Karkkainen, M. Halonen, K.A.I. , W-Band CMOS Amplifiers Achieving + 10 dBm Saturated Output Power and 7.5 dB NF, *IEEE JSSC*, Vol. 44, No. 12, Dec. 2009, pp 3403-3409.

[3] Yu-Sian Jiang Jeng-Han Tsai Huei Wang , A W-Band Medium Power Amplifier in 90 nm CMOS, *IEEE MWCL*, Vol. 18, No. 12, Dec. 2008, pp 818-820.

[4] Gilreath L, Jain V, Hsin-Cheng Yao, Le Zheng, Heydari, A Fully Integrated Auto-Calibrated Super-Regenerative Receiver in 0.13um CMOS, *IEEE JSSC*, Vol. 42, No 9, Sept. 2007, pp1976-1985.

[5] Adrian Tang and M. C. Frank Chang, 183GHz 13.5mW/Pixel CMOS Regenerative Receiver for mm-Wave Imaging Applications, *IEEE ISSCC 2011*, To be presented Feb 2011.

[6] Tomkins, P. Garcia and S. P. Voinigescu, A passive W-band imager in 65nm bulk CMOS,, *IEEE CSICS*, Oct. 2009, pp. 1-4.

[7] Tang, K.W, Khanpour M, Garcia P, Gamier, C, Voinigescu, S.P, 65-nm CMOS, W Band Receivers for Imaging Applications, *IEEE CICC*, Sept. 2007, pp 749-752.

[8] Gilreath L, Jain V, Hsin-Cheng Yao, Le Zheng, Heydari, A 94-GHz passive imaging receiver using a balanced LNA with embedded Dicke switch, *IEEE RFIC*, May 2010, pp 79-82.